ACTA ACUSTICA UNITED WITH ACUSTICA
Vol. 93 (2007) 435 – 446

Modelling the Mechanical Response of the Reed-Mouthpiece-Lip System of a Clarinet. Part II: A Lumped Model Approximation

Maarten van Walstijn
Queen's University Belfast, Sonic Arts Research Centre, Belfast BT7 1NN. m.vanwalstijn@qub.ac.uk

Federico Avanzini
University of Padova, Department of Information Engineering, Via Gradenigo 6/A, 35131 Padova, Italy. avanzini@dei.unipd.it

Summary
A non-linear lumped model of the reed-mouthpiece-lip system of a clarinet is formulated, in which the lumped parameters are derived from numerical experiments with a finite-difference simulation based on a distributed reed model. The effective stiffness per unit area is formulated as a function of the pressure signal driving the reed, in order to simulate the effects of the reed bending against the lay, and mass and damping terms are added as a first approximation to the dynamic behaviour of the reed. A discrete-time formulation is presented, and its response is compared to that of the distributed model. In addition, the lumped model is applied in the simulation of clarinet tones, enabling the analysis of the effects of using a pressure-dependent stiffness per unit area on sustained oscillations. The analysed effects and features are in qualitative agreement with players' experiences and experimental results obtained in prior studies.

PACS no. 43.75.Pq

1. Introduction

This study is aimed at developing a lumped model of the reed-mouthpiece-lip system of the clarinet, which can be applied in efficient and realistic simulation and synthesis of clarinet tones. Many authors (see for example [1, 2, 3, 4, 5, 6, 7]) have modelled the reed-mouthpiece-lip system as a linear one-mass system (see Figure 1). This approach stems from the idea that the reed can be considered as a clamped bar, of which only the lowest resonance is modelled in the one-mass model. Given the relatively strong damping of the higher reed resonances, this is a good first approximation of the dynamics of a freely vibrating reed (i.e., no further external forces are involved except the driving pressure). Moreover, the main component of the driving pressure is usually below the first reed resonance, so that considering a single mode tends to be sufficient in application to the simulation of clarinet tones. However, under real playing conditions the reed-mouthpiece-lip system is more complex than a simple clamped bar; the reed is supported by the lip, and "beats" against the mouthpiece lay during oscillation. The interaction with the lip, which provides extra damping but also shifts the natural reed resonance, is usually accounted for within the one-mass model by altering the lumped parameters, although reliable methods for experimental determination of these values appear not to be available. Beating is often modelled in a crude way, by simply imposing a maximum to the reed displacement (e.g., [8, 9]), thus assuming no reed-lay interaction up to that point. Little is known what the effects of this simplification is on the oscillations computed with such models. As beating is a strongly non-linear phenomenon, it can be expected to cause significant timbral shifts. It is therefore important to gain a better understanding of the effects of the reed-lay interaction on the oscillations produced with clarinets, especially with regard to sound synthesis applications.

Several studies have focussed on attempting to incorporate the effects of the non-linear interaction between the reed and the mouthpiece lay by means of a one-mass model with non-constant lumped parameters. Adrien *et al.* [10] (see [11] for more details) were among the first to take this approach. In their model, each of the lumped parameters is defined as a unique function of the reed opening. Although the authors claim that this method simulates the effect of the reed rolling on the mouthpiece lay, no theoretical or experimental method for determining the parameter functions is given. The first published attempt at developing a theoretical method for determining the parameter functions was made by Gazengel [12]. In that study, the lumped parameters are derived from a (continuous-time) distributed model of the reed. The main principle is based

Received 10 October 2006,
accepted 6 March 2007.

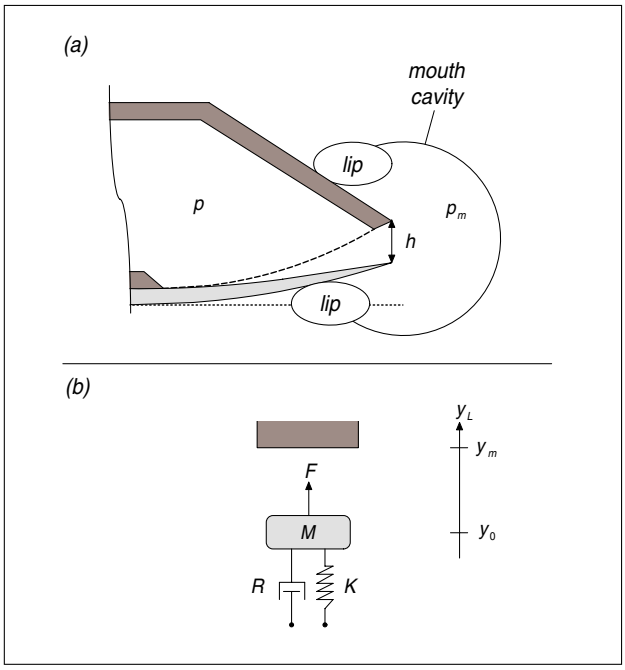

Figure 1. (a): Schematised view of a clarinet reed-mouthpiece-lip system. The dashed line indicates the profile of the mouthpiece lay, and p and p_m denote the mouthpiece pressure and the mouth pressure, respectively. (b): One-mass model of the reed tip vibration, with effective mass M, effective damping R, and stiffness K. The effective external force F exerted on the reed equals $S_d \Delta p$, where S_d is the effective driving surface, and $\Delta p = p_m - p$ is the pressure difference across the reed. The reed opening h is related to the reed tip position y_L by $h = y_m - y_L$, where y_m is the vertical position of the mouthpiece lay tip.

on the assumption that at each time instant, the lumped oscillator and the bar have equal potential and kinetic energies. This approach stems directly from Rayleigh's energy method for determining the eigenfrequencies of a beam under flexure such as explained in standard books on vibration theory (see for example [13, 14]), and has been applied previously in a musical acoustics context to determine the first resonance of an organ reed [15]. The main disadvantage of such an analytical approach is that the parameters can be derived only for idealised geometries of the reed and the mouthpiece lay. Gazengel [12] provides such results for a circular shaped mouthpiece lay curvature with a wedge-shaped reed clamped to it. Although this can provide some first insights into the global mechanical principles and functioning of the reed-mouthpiece-lip system, accurate parameter estimations that can be applied to realistic simulation of the sound production mechanism of an actual clarinet (as opposed to one with idealised geometries) cannot be obtained. This is because (1) the precise shape of the reed and the mouthpiece lay have a strong influence on the sound and the playing characteristics of the instrument, and (2) it is not clear how to incorporate the interaction with the lip in a verifiable manner.

An alternative is to use numerical simulations of the reed-mouthpiece-lip system, which are free from the geometrical limitations associated with the analytical approach. The numerical model can be employed as a "laboratory set-up" with which experiments can be run in a very controlled manner. This approach has already been used in a study by de Vries *et al.* [16] on the vocal folds, the lumped parameters of which were determined from numerical calculations with a finite-element model that is based on a precise set of geometrical and material data.

In the accompanying Part I of this paper [17], the reed-mouthpiece-lip system was modelled as a clamped bar, taking into account only transverse vibrations, and including the interaction with the lip and the lay. A numerical model was developed using finite difference methods, and the geometrical and material parameters were measured and estimated from a real reed and mouthpiece. The principal aim of the present study is to formulate a lumped model of the reed-mouthpiece-lip system that exhibits a vibrational behaviour that approximates that of the distributed model. The paper is structured as follows: in section 2, the non-linear lumped model is presented, starting from a quasi-static formulation. Section 3 then discusses the estimation of the parameters of the non-linear lumped model. In section 4, the non-linear lumped model is compared with the distributed model in terms of response to steady-state and transient driving signals. In section 5, a discrete-time model for simulation of clarinet tones is presented, and some of the effects of using a pressure-dependent stiffness per unit area in a lumped reed model are analysed. Finally some concluding remarks are presented in section 6.

2. Non-linear lumped model

2.1. Quasi-static model

The simplest possible lumped model of the clarinet reed-mouthpiece-lip system is obtained by regarding it as a system with stiffness only, neglecting any inertia or damping properties. This is often referred to as a quasi-static model, in which the reed moves in phase with the pressure driving it [18]. The equation of motion for this model is

$$K\,(y_L - y_0) = S_d \Delta p, \tag{1}$$

where K and S_d are the effective stiffness and driving surface, respectively, Δp is the pressure difference across the reed, y_L is the reed tip position, and y_0 is the equilibrium value of y_L. Because the strongest frequency components of sustained pressure driving signals in clarinets are usually well below the resonance frequency of the reed, the reed-mouthpiece-lip system can be regarded as "stiffness-dominated". It can be argued then that for simulation of sustained notes, the quasi-static reed model already forms a reasonably good approximation. However for oscillations in which the reed interacts with the lay, which occurs at medium and high playing levels, the lumped parameters K and S_d cannot be thought of as constant. In order to address this, the quasi-static model can be re-formulated with K and S_d as functions of Δp, such that it has the same static behaviour as the distributed model presented in Part

I. In such a formulation, it is more convenient to write the equation of motion more compactly as

$$K_a\{\Delta p\}\,(y_L - y_0) = \Delta p, \tag{2}$$

where

$$K_a\{\Delta p\} = \frac{K\{\Delta p\}}{S_d\{\Delta p\}} \tag{3}$$

is the stiffness per unit area. Nederveen [19] formulated a similar pressure-dependent reed model, in which the compliance function (the reciprocal of K_a) of the reed was determined experimentally. The pressure-dependent quasi-static formulation enables to model the reed response as a static non-linearity; this approach has been taken in several sound synthesis applications (for example in digital waveguide models of the clarinet [20, 21, 22]). In principle, the "reed-table" employed in these studies can be adapted to incorporate a measured non-linear dependency of K_a on Δp.

2.2. One-mass dynamic model

Having defined a quasi-static model with equation (2), the question arises to what extent the dynamic behaviour of the reed can be approximated with a lumped model. As mentioned in section 1, various previous studies have used a one-mass model in which all of the lumped parameters are functions of the reed tip displacement. In this approach, the reed is assumed to curl up to the mouthpiece lay in a smooth way; the effective mass can then be thought of as smoothly varying with the reed opening [10, 12]. However, as was demonstrated in Part I, the distributed model predicts more complicated dynamic behaviours, in which an area of the reed touches the lay before the part of the reed on the instrument-side of that area has come in contact with the lay (see also Figure 9 in Part I). This finding was qualitatively confirmed by the experiments on real reeds by Dalmont *et al.* [18]. As the reed moves towards closure, the tip of the reed will, at least for some period, move in a direction opposite to the point of the reed that has just been held in place by the inelastic collision with the mouthpiece lay. This type of motion of a clamped-free bar inherently involves additional contributions from one or more higher modes of vibration. Therefore, the resulting reed tip motion is *a priori* not well described by a one-mass model. Formulating the mass as a unique function of the reed tip position does not address this problem, since the instantaneous output of the model remains that of a single-mode system; a one-mass model is simply of the wrong order to simulate what is essentially multi-mode vibrational behaviour. Hence adding a single mass and damping term to equation (2) cannot serve the purpose of simulating all of the complex dynamic behaviour exhibited by the distributed model. Instead, its validity is limited to approximating the dynamic effects at small amplitudes, in which there is no significant reed-lay interaction. As will be demonstrated in section 3.2, it is reasonable to assume that the effective mass and damping are approximately constant for small-amplitude oscillations. Under this assumption, the equation of motion becomes

$$M_a\ddot{y}_L + R_a\dot{y}_L + K_a\{\Delta p\}\,(y_L - y_0) = \Delta p, \tag{4}$$

where $\dot{y}_L$ and $\ddot{y}_L$ denote reed tip velocity and acceleration, respectively, M_a is the mass per unit area, and R_a is the damping per unit area. Note that

$$R_a = M_a g, \tag{5}$$

where g is the reed damping, as used in many previous studies [2, 23, 5, 24].

2.3. Reed-induced flow

As the reeds oscillates, it is assumed to produce an air flow into the mouthpiece [4]:

$$u_r = S_r\{\Delta p\}\,\dot{y}_L, \tag{6}$$

where S_r is the flow-related effective surface. Although S_r is formulated starting from a different physical notion than the effective driving surface S_d in equation (1), and is indeed often treated as a different parameter [12, 11], it can be shown that the two formulations are in fact the same (see Appendix A1).

2.4. Discrete-time formulation

Computing time-domain reed responses with the non-linear lumped model requires discretising equation (4). For mathematical convenience, we first change to a variable with zero equilibrium:

$$M_a\ddot{\phi} + R_a\dot{\phi} + K_a\{\Delta p\}\phi = \Delta p, \tag{7}$$

where $\phi = y_L - y_0$ is the reed tip displacement. Given the variation of K_a with Δp, it is wise to choose a discretisation method that is unconditionally stable for any combination of physically feasible values of constant lumped parameters, so that the model cannot enter numerically unstable regions. A second important criterion is that the mapping from the analog to the digital domain is exact at $\omega = 0$, since the input driving pressure usually contains a strong DC component. Finally, we anticipate the use of the discrete-time reed oscillator in the full simulation of clarinet tones, in which it is advantageous to use a formulation with a zero instantaneous response; this way, an incomputable loop is avoided [25, 26]. Taking these criteria into account, the impulse invariant method [27] is a good candidate, with additional amplitude scaling to ensure the exactness of the mapping at DC. This yields the difference equation:

$$\begin{aligned}\phi(n+1) = {} & b_1\{\Delta p(n)\}\,\Delta p(n) \\ & - a_1\{\Delta p(n)\}\,\phi(n) \\ & - a_2\,\phi(n-1),\end{aligned} \tag{8}$$

where for a sample period T, we have

$$a_2 = \mathrm{e}^{-gT}, \tag{9}$$

and where the values of the coefficients a_1 and b_1 are obtained for each time step n via interpolation of look-up tables, the stored values of which are defined as

$$\begin{aligned} a_1\{\Delta p(n)\} &= -2\mathrm{e}^{-gT/2}\cos\left(\omega_r^2\{\Delta p(n)\}T\right), \\ b_1\{\Delta p(n)\} &= \frac{1 + a_1\{\Delta p(n)\} + a_2}{K_a\{\Delta p(n)\}}, \end{aligned} \tag{10}$$

where

$$\omega_r^2\{\Delta p(n)\} = \sqrt{\frac{K_a\{\Delta p(n)\}}{M_a} - \frac{g^2}{4}}. \tag{11}$$

For any constant value of K_a, we can compute the frequency response of the discrete-time reed model. Figure 2 compares the discrete-time model to the (ideal) continuous-time model in terms of amplitude response, for four different K_a values (chosen within the expected range of variation), using a 44.1 kHz sample rate. In the computations, M_a and R_a were set to the values estimated from the distributed model, as will be described in section 3. The main drawback of the impulse invariant method is that it causes aliasing effects [27], which is reflected in Figure 2 in that high frequency components are less accurately modelled than low frequency components. Given that the reed response is low-pass, and that the reed is mainly driven at low frequencies, these effects are not significant as long as a sufficiently high sample rate is chosen. Of course in the real system, K_a varies during oscillation, and a frequency response cannot be defined. Nevertheless the plot provides a first indication that the effects of discretisation are small at 44.1 kHz sample rate.

Although the impulse invariant method is unconditionally stable for discretisation of linear systems, stability conditions are not as easily determined for the non-linear system at hand, especially given that the non-linearity is not analytically described. However, no stability problems were encountered during our simulations.

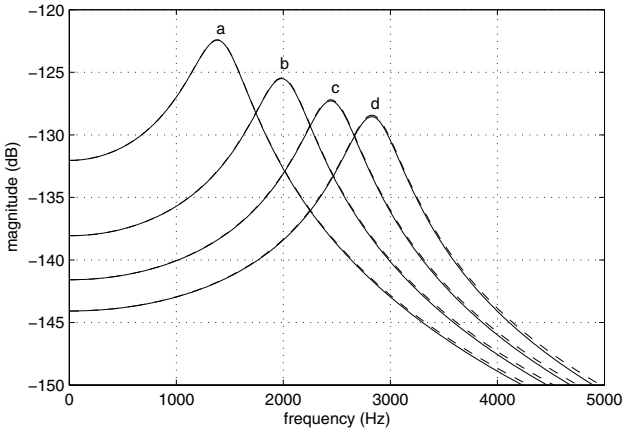

Figure 2. Reed frequency response, for 4 different values of effective stiffness. For the curves a, b, c, and d, the respective values are K_a =4, 8, 12, and 16 MN m^{-3}. The solid lines indicate the analog responses, and the dashed lines indicate the digital responses. A 44.1 kHz sample rate was used. The y-axis displays the magnitude on a logarithmic scale, that is calculated as 20 $\log_{10}|H(f)|$, where $H(f)$ is the complex frequency response at frequency f.

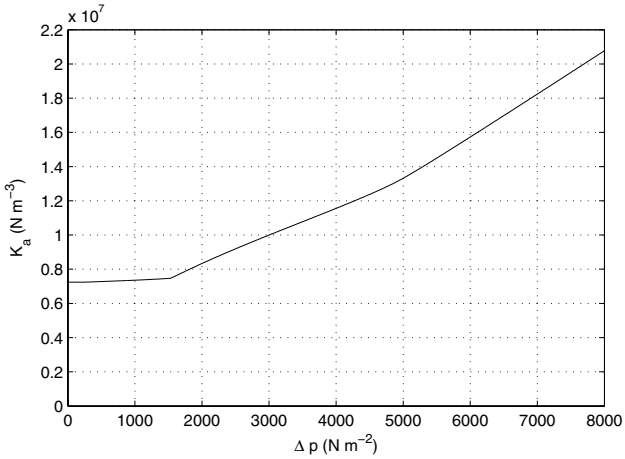

Figure 3. Effective stiffness per unit area as a function of pressure difference, as derived from static simulations with the distributed model.

3. Lumped parameter estimation

3.1. Estimation from static simulations

3.1.1. Effective stiffness per unit area

As explained in Part I, the dependence of K_a on the reed tip position can be derived from equation (2), using a series of static numerical simulations with the distributed model to provide the values of y_L and Δp. As described in section 4 of Part I, the parameters of the numerical simulation were determined via measurements on a Rico Plasticover reed (hardness 2) and a Bundy mouthpiece. The parameter K_a was derived in Part I using a finite difference model using two hundred reed sections. Figure 3 shows K_a as a function of Δp, as derived from a simulation using one thousand reed sections; the higher spatial resolution was chosen in order to reduce the numerical artefacts introduced by spatial discretisation of the mouthpiece lay shape.

3.1.2. Effective Reed Surface

The static simulations with the distributed model can also be used to estimate how the effective reed surface varies with Δp. This is done here using the two different formulations, S_r and S_d.

The full equation of motion for the reed-mouthpiece-lip system is given by equation (1) in Part I. Under quasi-static conditions, damping and mass terms are ignored, and all time-varying variables can be regarded as being unique functions of Δp. The equation of motion can then be written

$$\begin{aligned} \frac{\partial^2}{\partial x^2}\left[Y\,I(x)\frac{\partial^2 y}{\partial x^2}(x,\Delta p)\right] &= F_{ext}(x,\Delta p) \\ &= +F_{lip}(x,\Delta p) \\ &= +F_{lay}(x,\Delta p), \end{aligned} \tag{12}$$

where $F_{ext} = w\Delta p$ is the driving force per unit length (w is the width of the reed), and F_{lip} and F_{lay} are force terms representing the interaction with the lip and the lay, respectively. In the following, we will suppress in our notation the dependence of variables on Δp. For example, the "reed state" will be written as $y(x)$.

Regarding the lumped model, we can define the volume of air V that is displaced by moving from equilibrium state $y_0(x)$ to $y(x)$:

$$V = w \int_0^L [y(x) - y_0(x)]\, \mathrm{d}x, \tag{13}$$

where L is the length of the reed. Now combining the fact that $u_r = \dot{V}$ with equation (6) allows to deduce that

$$S_r\{\Delta p\} = \frac{\dot{V}}{\dot{y}_L} = \frac{\mathrm{d}V}{\mathrm{d}y_L}. \tag{14}$$

Hence the effective surface S_r can be calculated as a function of Δp by first computing and storing both V and the reed tip position y_L for a range of pressure difference values, and numerically computing the derivative $\mathrm{d}V/\mathrm{d}y_L$.

The formulation of S_d is more elaborate, and is based on the principle that the potential energies of the distributed and the lumped model should be equal for all static reed states. The potential energy of the distributed model is

$$E_p = E_r + E_{lip} + E_{lay} - E_0, \tag{15}$$

where

$$E_r = \frac{1}{2} \int_0^L Y I(x) \left(\frac{\partial^2 y}{\partial x^2}(x) \right)^2 \mathrm{d}x \tag{16}$$

is the potential energy stored in the reed,

$$E_{lip} = \frac{1}{2} K_{lip} \int_0^L \Delta y_{lip}^2(x)\, \mathrm{d}x \tag{17}$$

is the energy stored in the lip,

$$E_{lay} = \frac{1}{2} K_{lay} \int_0^L \Delta y_{lay}^2(x)\, \mathrm{d}x \tag{18}$$

is the energy stored in the lay, and

$$E_0 = \left[E_r + E_{lip} + E_{lay} \right]_{\Delta p = 0} \tag{19}$$

is a term included to ensure that $E_p = 0$ at equilibrium. In the above equations, K_{lip} and K_{lay} are the effective stiffnesses per unit length of the lip and the mouthpiece lay, respectively, associated with the compression terms $\Delta y_{lip}(x)$ and $\Delta y_{lay}(x)$ (see section 2 in Part I for more detailed descriptions). The potential energy of the distributed model can be calculated from the finite difference simulation results using numerical versions of equations (16), (17), and (18).

In the lumped model, the infinitesimal variation of potential energy dE_p is the product of the effective elastic force $K\Delta p(y_L - y_0)$ and the infinitesimal displacement dy_L, hence we have

$$\frac{\mathrm{d}E_p}{dy_L} = K\{\Delta p\}\,(y_L - y_{L0})\,. \tag{20}$$

Combining equations (20), (2), and (3) gives

$$S_d\{\Delta p\} = \frac{\left(\dfrac{\mathrm{d}E_p}{dy_L} \right)}{\Delta p}. \tag{21}$$

Thus S_d can be estimated by first computing the potential energy for a set of reed states (using the distributed model), numerically calculating the derivative with respect to y_L, and then dividing by Δp.

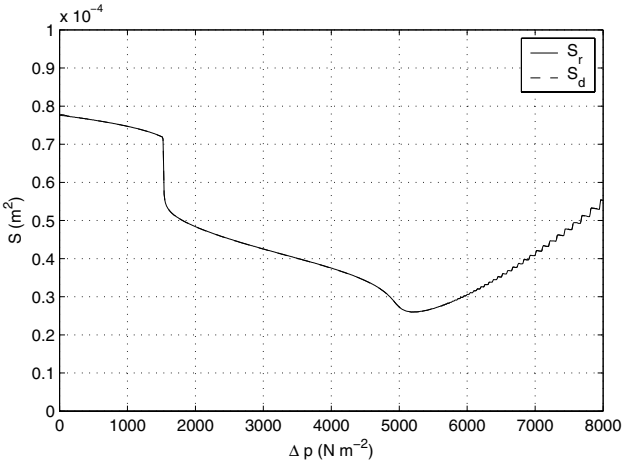

Figure 4. Effective surface as a function of pressure difference, as derived from static simulations with the distributed model. Note that the curves of S_r (solid) and S_d (dashed) almost entirely overlap.

Figure 4 shows S_r and S_d as a functions of Δp. The plots confirm the equality of the two effective reed surface formulations (see Appendix A1 for an analytic proof). The curves in Figure 4 exhibit a sudden jump at about $\Delta p = 1550\,\mathrm{N\,m^{-2}}$, and at the same point the curve in Figure 3 undergoes a jump in its first derivative; these discontinuities coincide with the jump in "separation point" explained in section 5.3. of Part I. The staircase-like shape of the plot in Figure 4 for large values of Δp is due to the discretisation of the mouthpiece lay. That is, in the numerical model, the lay does not present a smooth curving boundary, but rather a stepped one, which results in small step-wise variations of the variables used in the derivation of S_r and S_d. This numerical artefact is neglible for small values of Δp, and can be generally reduced by choosing a higher spatial resolution in the numerical implementation of the distributed model.

3.2. Estimation from dynamic simulations

The main advantage of including a mass and a damping term is that it allows more realistic simulation of transients, in which there is often some excitation of the reed resonance. In addition, damping and inertia play a key role

in the transition to the clarion register [3, 4]. The effective mass per unit area for small-amplitude oscillations can be derived from dynamic simulations with the distributed model. For this purpose, the distributed model was excited with ten different transient signals of the form of a constant pressure Δp_c plus a short, small-amplitude impulsive signal in the shape of a Hanning window of 0.5 ms. For each simulation, first the constant pressure value was applied. The Hanning pulse was then applied after the initial transient had decayed. The ten different constant pressure values were chosen in the area around the predicted threshold blowing pressure of approximately $1000\,\mathrm{N\,m^{-2}}$. The added constant pressure values allow to investigate the inertia effects in the pressure range in which the reed resonance is most likely to be excited under normal playing conditions. For each simulation, the output signals resulting from the Hanning pulse excitation were analysed in terms of resonance frequency and reed damping; this was done by fitting the frequency-domain response of an analytic harmonic oscillator model to that of the measured data. Figure 5 shows the resulting estimated values. As can be seen from the plots, both the resonance frequency and the damping coefficient vary only marginally with Δp within the pressure range around threshold. Hence for small oscillations, we may define an angular resonance frequency $\omega_r = 2\pi f_r$, that is related to the lumped parameters by

$$\omega_r^2 = \frac{K_a}{M_a} \tag{22}$$

Since the variation of K_a with Δp is extremely small for small driving oscillations around $1000\,\mathrm{N\,m^{-2}}$ (see Figure 3), it follows from equation (22) that the effective mass per unit area M_a does not vary significantly in this range either, and approximately takes on the value

$$M_a = K_a(1000)/\bar{\omega}_r^2 \approx 0.05\ \mathrm{Kg\ m^{-2}}, \tag{23}$$

where $\bar{\omega}_r$ is the mean value over the measured resonance values. Note that our estimate of M_a is about twice the value of $0.0231\,\mathrm{Kg\,m^{-2}}$ estimated by Worman [2]. Worman's estimate of K_a was effectively about $1.24 \times 10^7\,\mathrm{N\,m^{-3}}$, so within the same range as the function plotted in Figure 3, but higher than the value near threshold or equilibrium. Of course, the estimated lumped parameter values depend on the particular reed and lay shapes, as well as the embouchure, so some discrepancies are to be expected.

The damping parameter R_a is not estimated here; in Part I, the damping parameters of the distributed model were fine-tuned such that the numerical simulation results exhibited a small-amplitude damping behaviour that matches with $g \approx 2900\,\mathrm{s^{-1}}$ at its first resonance, similar to the value found empirically by Worman. Hence for the lumped model, we simply set $R_a = 2900 M_a$.

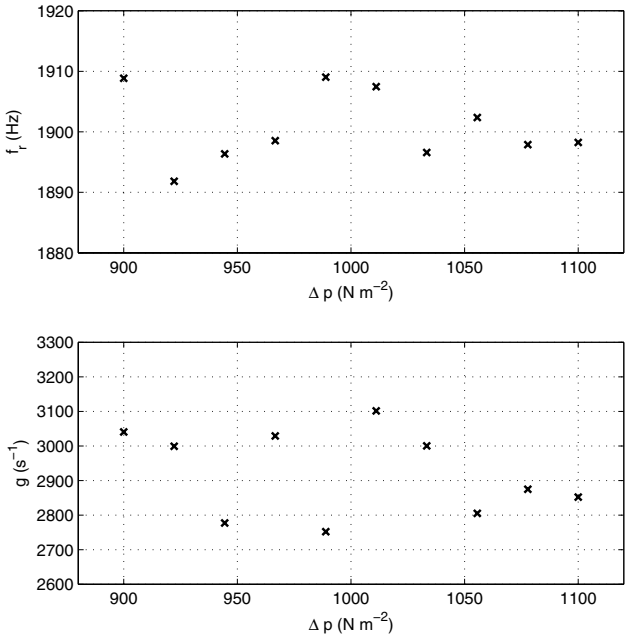

Figure 5. Estimation of the reed resonance frequency (top) and reed damping (bottom), from ten transient simulations with the distributed model. For each simulation, the driving pressure signal consisted of a constant value plus a Hanning pulse.

4. Response Comparisons

4.1. Steady-state response

In order to compare the non-linear one-mass dynamic reed model and the distributed model for steady-state input signals, both were driven with a pressure difference signal of the form:

$$\Delta p(t) = A_d\,[1 + \sin(2\pi f_d t)]\,, \tag{24}$$

where A_d and f_d are the driving amplitude and frequency, respectively. The DC-offset is included so that the signal more closely resembles pressure difference signals typically observed in real clarinets. In order to get insight into the effects of using a pressure-dependent K_a, the same signal was also applied to a lumped model with a constant stiffness per unit area (set to the equilibrium value) and "abrupt" inelastic beating, such as in [8, 9]. In other words, the second lumped model is described by

$$\begin{aligned} &\text{if} \quad y_L < y_m : \\ &\qquad M_a \ddot{y}_L + R_a \dot{y}_L + K_a\,(y_L - y_0) = \Delta p, \\ &\text{otherwise:} \\ &\qquad y_L = y_m, \quad \dot{y} = 0, \end{aligned} \tag{25}$$

where y_m is the maximum reed tip position. This formulation can be discretised in the same way as equation (4), but in this case results in a difference equation with constant coefficients. Figure 6 shows the respective outputs for a set of driving signals with different combinations of amplitude ($A_d = 500, 1500, 3000, 4500\,\mathrm{N\,m^{-2}}$) and frequency ($f_d = 200, 1000, 1600\,\mathrm{Hz}$). As can be seen from

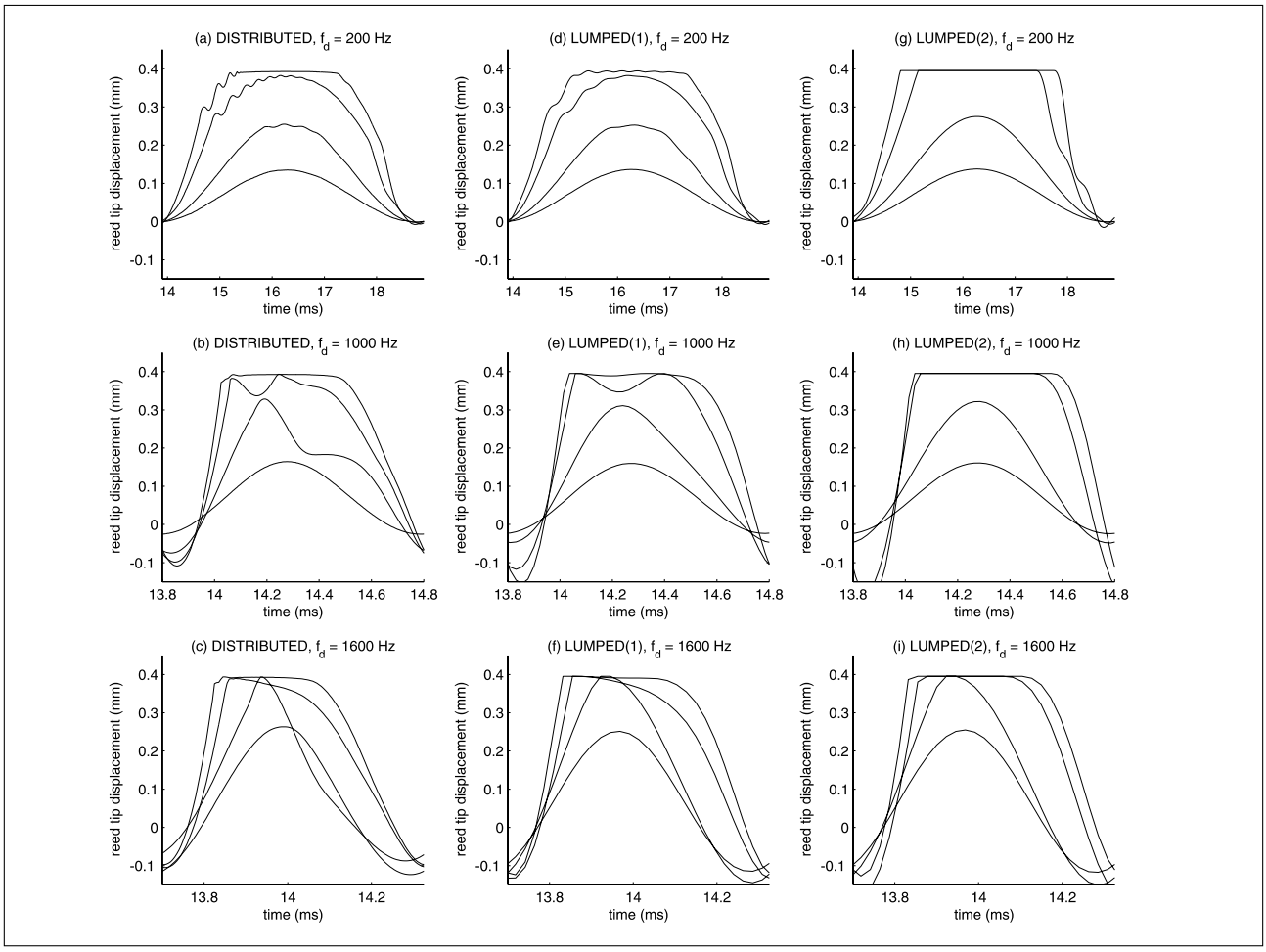

Figure 6. Steady-state comparison between the distributed model, the lumped model with pressure-dependent K_a [lumped (1)], and the lumped model with abrupt beating [lumped(2)], for different driving frequencies and amplitudes. For each driving frequency, exactly one period is plotted.

the plots, the results produced with the lumped model with pressure dependent K_a are very similar to the outputs of the distributed model. The main discrepancies occur with $f_d = 1000\,\mathrm{Hz}$, when driven at medium amplitude levels (see Figures 6b and 6e). The distributed model then exhibits a more complex behaviour in which the reed tip temporarily swings back in the opposite direction, as discussed in the introduction.

For small-amplitude driving signals, the second lumped model also produces results similar to those produced with the distributed model. This could be expected, since there is no significant reed-lay interaction in that case. However for medium-amplitude driving signals, the second lumped model consistently yields significantly different waveforms. At low driving frequencies, the second lumped model also exhibits significant discrepancies for large-amplitude driving signals (see Figures 6a and 6g). That is, "fully beating" is also a regime that is not well described with the second lumped model.

4.2. Transient response

The transient response of the lumped model can be tested in a similar way as with the analysis of resonance and damping properties in section 3.2, i.e., using a short Hanning pulse excitation, but in this case without an added constant value. Figure 7 compares the Hanning pulse response of the lumped model to that of the distributed model; the close match indicates the correctness of the effective mass estimate. We note that, as discussed in the

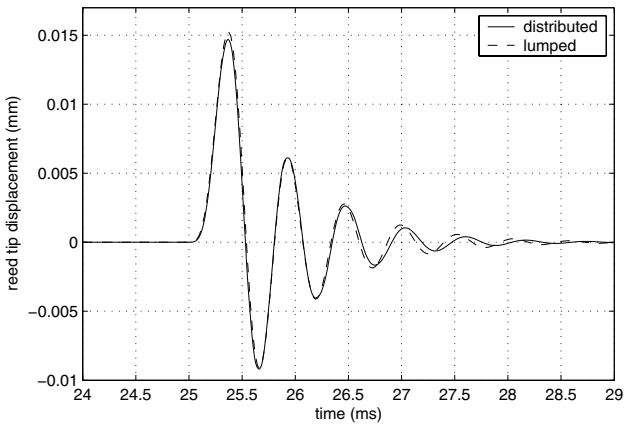

Figure 7. Response of the reed to a short pulse.

introduction, the lumped model only approximates the dynamic behaviour of the distributed model for small-amplitude oscillations.

5. Simulation of clarinet tones

5.1. Modelling the coupled system

A simplified clarinet -in the form of an open-ended, 40cm long cylindrical main duct with a radius of 6.5mm, connected to a conical and a cylindrical section that model the mouthpiece -was simulated in the discrete-time domain using the wave digital modelling (WDM) approach outlined in [28]. The wave digital model performs an operation that is equivalent to calculating the in-going wave p^- via linear convolution of the out-going wave p^+ with an approximation r_f of the aircolumn reflection function:

$$p^- = r_f * p^+. \tag{26}$$

When the aircolumn is coupled to the reed, the system can be driven into periodic sustained oscillations at frequencies near the aircolumn resonance frequencies, in which case there is an oscillating volume flow u_f through the reed channel. Following the studies in [7, 29, 9], this flow is assumed to obey:

$$\Delta p = p_m - p = \mathrm{sign}(u_f) \cdot \frac{\rho}{2} \left(\frac{u_f}{w\, h} \right)^2, \tag{27}$$

where $h = y_m - y_L$ is the reed opening. The sign of the volume flow is included such that the flow can become both positive and negative. The total flow into the mouthpiece is calculated as the sum of the flow u_f entering through the reed channel and the flow u_r that is induced by the motion of the reed (see equation (6)):

$$u = u_f + u_r, \tag{28}$$

and the pressure and volume flow at the reed are assumed to be a superposition of the in-going and out-going waves:

$$p = p^+ + p^-, \tag{29}$$
$$Z_0\, u = p^+ - p^-, \tag{30}$$

where Z_0 is the characteristic impedance at the mouthpiece entry. In combination with equations (6) and (4), the above equations describe the complete coupled system. A numerical formulation of this system is given in Appendix A2.

5.2. Properties of the simplified clarinet

The simplified clarinet described above contains two non-linearities, namely the fluid-dynamical non-linear relation between u_f, p, and h in equation (27), plus a second, purely mechanical non-linearity that is introduced with the use of a pressure-dependent stiffness per unit area. The simulation of the simplified clarinet can be used in order to investigate various effects that the mechanical non-linearity has on the production of sustained oscillations. Three specific features are addressed here. First, the flow versus pressure difference behaviour is analysed. This provides some initial clues about the basic properties such as threshold pressure [30]. The second feature that is analysed is the dependency of the playing frequency on the mouth pressure. Finally, the spectral evolution of the mouthpiece pressure waveform for an increasing mouth pressure is calculated. This gives insight to how the mechanical non-linearity influences the timbre of the sound produced by the simplified clarinet.

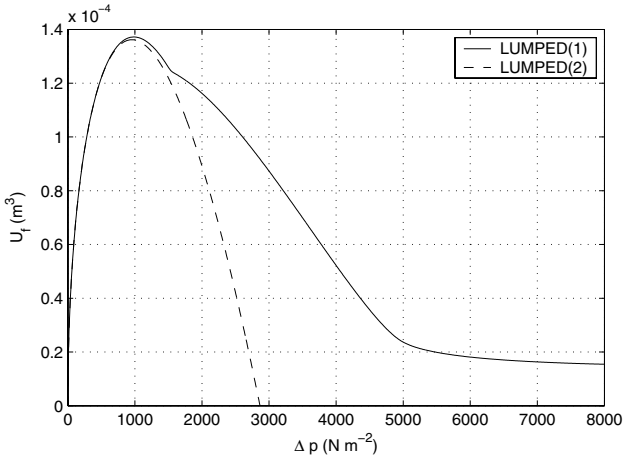

Figure 8. Volume flow versus pressure difference, as calculated for the lumped model under quasi-static conditions, using a formulation with pressure-dependent stiffness per unit area [lumped (1)], and a formulation with constant stiffness per unit area and abrupt beating [lumped(2)].

5.2.1. Volume flow versus pressure difference

The flow versus pressure difference curve is usually obtained by measuring or calculating the amount of flow through the reed channel under static conditions (i.e., without reed oscillation), for a range of pressure differences. The relation between pressure difference and flow obtained this way also holds for quasi-static conditions (i.e., when the reed is assumed to move exactly in phase with the pressure difference) [7]. For the simplified clarinet model, the curve can be computed directly, by first inverting equation (27), and then combining with equation (2) to eliminate y_L, which for $\Delta p \geq 0$ yields

$$u_f = w \left[y_m - y_0 - \frac{\Delta p}{K_a(\Delta p)} \right] \sqrt{\frac{2\Delta p}{\rho}}. \tag{31}$$

Figure 8 compares the computed curves for the two lumped models (one with pressure-dependent stiffness per unit area and one with abrupt beating). The shape of the curve depends heavily on the stiffness of the reed [31], as well as on the interaction with the lip and the lay. Hence we stress that there is by no means a "definitive" curve, but rather a set of curves that depend on the properties of the reed, the player's embouchure, and the mouthpiece lay. With regard to comparing the two lumped models, the curve maxima

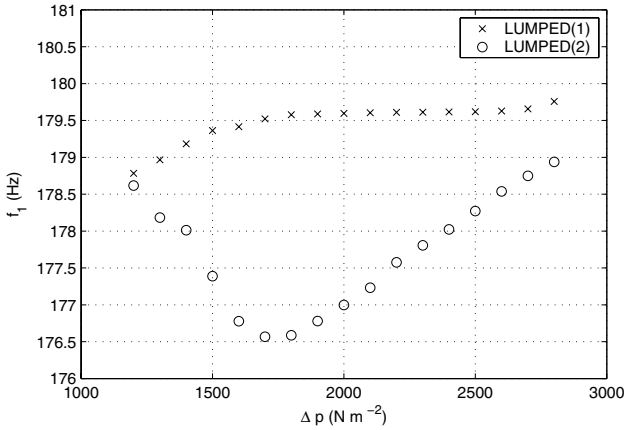

Figure 9. Playing frequency as a function of mouth pressure. All data-points were calculated using FFT-analysis of the waveforms obtained by running the simulation with a constant mouth pressure. Plotted are the results obtained with the lumped model with pressure-dependent stiffness per unit area [lumped(1)], and with the lumped model with abrupt beating [lumped(2)].

are very close, thus it can be expected that the values of the threshold pressure differences (which lie closely near the maxima, on the right side [31]) are very similar. On the other hand, the pressure difference at which the reed fully closes (i.e., $u_f = 0$) is much larger for the first lumped model. In other words, when using a pressure-dependent stiffness per unit area, there is a much wider mouth pressure range for which sustained oscillations can be produced; this finding is in qualitative agreement with measurements by Dalmont *et al.* [18].

5.2.2. Playing frequency versus mouth pressure

Experiments with a mechanically blown clarinet by Bak and Dømler [32] have shown that in real clarinets, the playing frequency is positively correlated to the mouth pressure. Although for small-amplitude oscillations, this dependence can to some extent also be explained in terms of hydrodynamic effects [7], most of the dependence is due to the changing flexibility of the reed [32, 7]. In order to investigate this dependence for the reed-mouthpiece-lip system simulated in the current study, the two lumped models were applied in simulations with feedback from the bore, and subsequently the fundamental frequency of each the resulting sustained oscillations was estimated using an FFT in combination with a second-order interpolation routine in order to obtain a higher frequency resolution. The resulting data is plotted in Figure 9. Using a pressure-dependent stiffness per unit area, the playing frequency gradually increases with mouth pressure, whereas the use of a constant stiffness per unit area and abrupt beating results in a noticeable dip in frequency. A small gradual rise with mouth pressure of about 20 cents over a pressure range of $1600\,\mathrm{N\,m^{-1}}$, as found with the first lumped model, is in fact quantitatively similar to the experimental results obtained by Bak and Dømler.

5.2.3. Spectral Evolution

The mechanical non-linearity of the reed may also be expected to have considerable effects on the spectral evolution of the radiated sound. In order to investigate these effects, a slowly increasing mouth pressure was applied in the simulation. Figure 10 depicts the resulting mouthpiece pressure spectrograms. After a short period of constant mouth pressure, it was linearly increased from 1100 to $4000\,\mathrm{N\,m^{-2}}$ over a period of 4.5 seconds, and then quickly reduced to the starting value.

When a constant stiffness per unit area is used, the spectrum does, apart from the dip in pitch, not show much change after the reed has started beating (at about $t = 0.25$ s). That is, at the point where the reed starts to beat, many partials are immediately produced, and thereafter the spectrum is only very marginally slightly affected by the gradual increase in mouth pressure. On the other hand, when employing a pressure-dependent stiffness per unit area there is clearly a gradual rise of higher harmonics during the period of increasing mouth pressure, i.e., the spectral content is a smooth function of the mouth pressure. The latter finding is in qualitative agreement with the experience of clarinettists that with a given embouchure, blowing softer produces a "mellow" tone while blowing harder produces a "bright" tone. Such timbral shifts in real clarinets can also explained by non-linear propagation effects in the air column [33], but these can be expected only to become significant at high playing levels. Hence the results indicate that the reed-lay interaction can be a significant factor in the correlation between mouthpiece pressure and timbre.

6. Conclusions

In this paper we have proposed a method for inclusion of the effects of the reed-lay interaction in a lumped oscillator model of the reed-mouthpiece-lip system. A non-linear lumped model was presented, in which the stiffness per unit area is a pressure-dependent parameter. This way, the lumped model can be defined to have exactly the same static behaviour as the distributed model presented in the accompanying paper [17]. Methods for estimating the parameters of the non-linear lumped model were presented, using both static and dynamic simulations with the distributed model.

A discrete-time formulation of the non-linear lumped model was developed and used to demonstrate that it closely approximates the vibrational behaviour of the distributed model, with exception to cases in which the distributed model exhibits oscillations that involve significant contributions from the higher modes of the reed. In many previous studies, the lumped model is formulated using a constant stiffness per unit area, and reed beating is modelled as an "abrupt cap" on the reed position. Time-domain simulations with this second lumped model shows that it only approximates the distributed model for small-amplitude regimes, in which there is no significant reed-lay interaction.

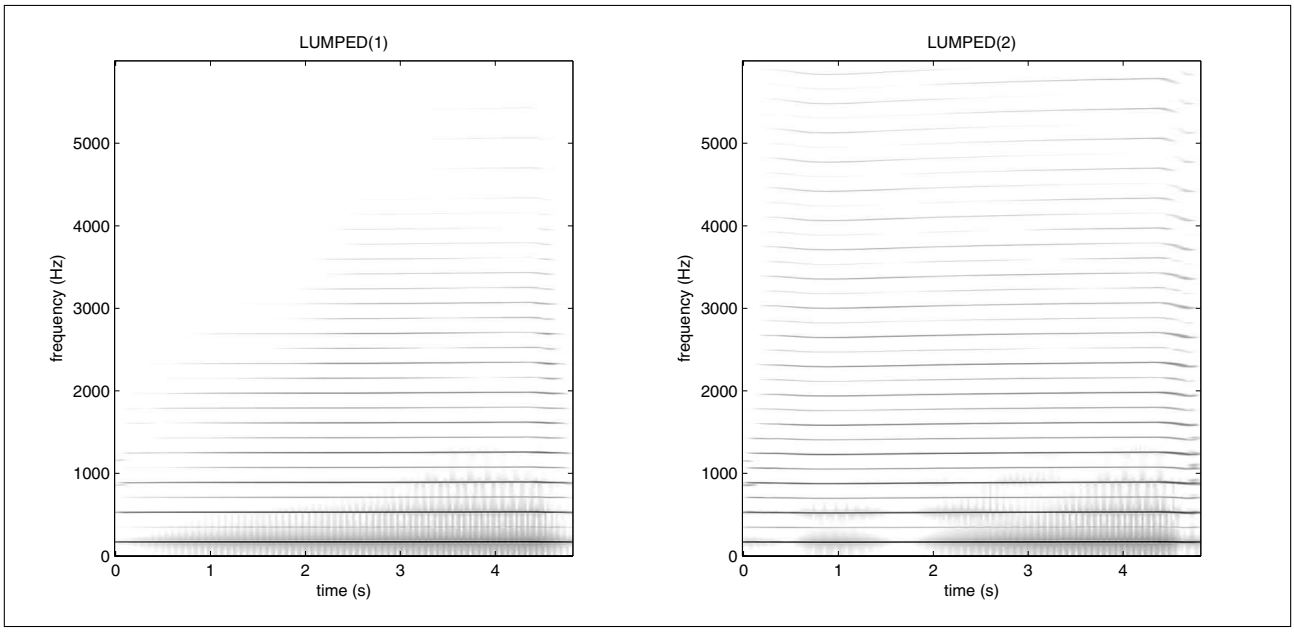

Figure 10. Spectrograms of the mouthpiece pressure, as computed with the fully coupled system, using a lumped model with a pressure dependent stiffness per unit area [lumped(1)], and with constant parameters and abrupt beating [lumped(2)]. The mouth pressure was linearly increased from 1100 N/m^2 to 4000 N/m^2, and then quickly reduced to 1100 N/m^2. An 44.1 kHz sample rate was used.

The non-linear lumped model of the reed-mouthpiece-lip system enables us to investigate the influence that the phenomenon of the reed bending against the lay has on the sound and playing characteristics of a clarinet. Using a simplified model of the air column (that is, an open-ended cylindrical duct with a mouthpiece), a time-domain simulation of a clarinet-like instrument that produces sustained oscillations was formulated. This simulation was run with the two different lumped models mentioned above. The results show that the formulation with pressure-dependent stiffness unit per area exhibits (1) a positive correlation between playing frequency and mouth pressure that is of the same order as previously found via experiments by Bak and Dømler [32], and (2) a smooth growth of higher partials with increasing mouth pressure, which is in qualitative agreement with players' experiences. Moreover, the sustained oscillations resulting when using a lumped model with "abrupt beating" are significantly different.

It must be noted that our results are based only on a numerical simulation of a clarinet-like system, and more definite conclusions concerning the effects of the reed-lay interaction can only be made after thorough comparison between simulations and experiments with real clarinets. Moreover, all simulations use a particular mouthpiece, reed, and "embouchure". Hence drawing more general conclusions would require to apply numerical experiments to a wider variety of system and parameter configurations. Another improvement would be to use a 2D rather than a 1D distributed model, so that the influence of the first torsional mode – that has recently been related to musical quality [34] – can be taken into account. We envisage that such laboratory and numerical experiments would form the logical next steps to undertake in future work on this subject.

Finally, we would like to point out that the work presented here has direct implications for musical sound synthesis. As shown in section 5.2, varying the mouth pressure corresponds to changing the amplitudes of the higher harmonics of the generated oscillations. This feature is typically aimed for in the context of sound synthesis via physical modelling; it allows for the same kind of natural and intuitive timbre control that is exerted by the player of a real woodwind instrument. Development of a full, musically useful sound synthesis model will however require more research, since it would inevitably involve the parameterisation of embouchure changes.

Appendix

A1. Equality of S_r and S_d

The effective surface formulations S_r and S_d are given in equations (14) and (21), respectively. These equations hold under quasi-static conditions, and the equation of motion for the distributed model is then given by equation (12). There are no losses and the kinetic energy is zero at all times, hence all the energy in the system consists of potential energy. Of the forces acting on the reed, F_{lip} and F_{lay} are passive restoring forces, while $F_{ext} = w\Delta_p$ is the external driving force that supplies energy into the system. It follows that the work done through F_{ext} must equal the change in potential energy.

Consider now that due to the supplied driving force per unit length, the reed moves a small amount from $y(x) - \mathrm{d}y(x)$ to $y(x)$. The work per unit length done at position x is thus

$$W(x) = F_{ext}(x)\,\mathrm{d}y(x) = w\,\Delta p\,\mathrm{d}y(x). \qquad \text{(A1)}$$

The infinitesimal change in potential energy of the system is

$$\begin{aligned} \mathrm{d}E_p &= \int_0^L W(x)\,\mathrm{d}x = \int_0^L w\,\Delta p\,\mathrm{d}y(x)\,\mathrm{d}x \\ &= \Delta p\,\left[w\int_0^L \mathrm{d}y(x)\,\mathrm{d}x\right] = \Delta p\,\mathrm{d}V, \end{aligned} \tag{A2}$$

where

$$\mathrm{d}V = w\int_0^L \mathrm{d}y(x)\,\mathrm{d}x \tag{A3}$$

is the infinitesimal amount of volume displaced by moving the reed by $\mathrm{d}y(x)$. Equation (A2) can be rewritten to obtain:

$$\frac{\left(\dfrac{\mathrm{d}E_p}{dy_L}\right)}{\Delta p} = \frac{\mathrm{d}V}{dy_L}. \tag{A4}$$

Now substituting equation (21) at the left-hand side and equation (14) at the right-hand side gives

$$S_d\{\Delta p\} = S_r\{\Delta p\}. \tag{A5}$$

A2. Numerical formulation of the coupled system

The objective is to solve the system of equations

$$\begin{aligned} \Delta p(t) &= M_a\ddot{\phi}(t) + R_a\dot{\phi}(t), \\ &= +K_a\{\Delta p(t)\}\phi(t), && \text{(A6)}\\ y_L(t) &= \phi(t) + y_0 && \text{(A7)}\\ h(t) &= y_m - y_L(t), && \text{(A8)}\\ u_r(t) &= S\{\Delta p(t)\}\,\dot{y}_L, && \text{(A9)}\\ p^-(t) &= \left(r_f * p^+\right)(t), && \text{(A10)}\\ p_m(t) - p(t) &= \mathrm{sign}[u_f(t)]\,\frac{\rho}{2}\left[\frac{u_f(t)}{w\,h(t)}\right]^2, && \text{(A11)}\\ u(t) &= u_f(t) + u_r(t), && \text{(A12)}\\ p(t) &= p^+(t) + p^-(t), && \text{(A13)}\\ Z_0\,u(t) &= p^+(t) - p^-(t), && \text{(A14)}\\ \Delta p(t) &= p_m(t) - p(t) && \text{(A15)} \end{aligned}$$

at the "new" discrete-time instant $t = (n+1)T$, knowing all the variables at the previous time instants. As explained in section 2.4, equation (A6) is discretised using a scaled version of the impulse invariant method, which yields equation (8) that enables the new reed displacement $\phi(n+1)$ to be computed from the pressure difference $\Delta p(n)$ at the previous time-instant. The new reed position $y_L(n+1)$ and opening $h(n+1)$ are then computed using equation (A7) and (A8). If $h(n+1)$ becomes negative, it is set to a value close to zero. The new reed-induced flow is now obtained by discretising equation (A9) using the backward Euler rule,

$$u_r(n+1) = S\left[\frac{y_L(n+1) - y_L(n)}{T}\right], \tag{A16}$$

where the effective surface S is now taken as a constant equal to the value estimated for S_r near equilibrium. This simplification has only a marginal effect on the solution of the system; this was checked by comparing the reed-induced flow output of the lumped model to that of the distributed model, which gave very similar results. Next, we seek to obtain $u_f(n+1)$. Combining equations (A11), (A12), (A13) and (A14) yields

$$\sigma(n+1)\,\frac{\rho}{2}\left[\frac{u_f(n+1)}{w\,h(n+1)}\right]^2 = \tag{A17}$$

$$p_m(n+1) - Z_0 u_f(n+1) - Z_0 u_r(n+1) - 2p^-(n+1),$$

$$\text{where}\quad \sigma(n+1) = \mathrm{sign}[u_f(n+1)]. \tag{A18}$$

This is a non-linear equation in $u_f(n+1)$ that can be written

$$D_1\,\sigma\,\left[u_f(n+1)\right]^2 + D_2\,u_f(n+1) + D_3 = 0, \tag{A19}$$

where D_1, D_2 and D_3 are temporarily considered as constants within each time step,

$$\begin{aligned} D_1 &= \frac{\rho}{2\,[w\,h(n+1)]^2}, && \text{(A20)}\\ D_1 &= Z_0, && \text{(A21)}\\ D_3 &= 2p^-(n+1) - p_m(n+1) \\ &\quad + Z_0\,u_r(n+1). && \text{(A22)} \end{aligned}$$

Because the wave digital model of the simplified clarinet employs a bidirectional delay-line to model the cylindrical entry section of the mouthpiece [28], the new value of the reflected wave $p^-(n+1)$ can be obtained simply from the lower delay-line of the model. Equation (A19) is now solved using the Newton-Raphson method. The function for which the root is solved is monotonic under all circumstances, thus equation (A19) always has a single, unique solution. Using the previous value $u_f(n)$ as the initial value for the iteration, it was found that nine iterations are typically sufficient for an accurate solution of the non-linear equation. The new volume flow $u(n+1)$ into the instrument is now obtained via equation (A12), and is used to calculate the current in-going wave via equation (A14),

$$p^+(n+1) = p^-(n+1) + Z_0\,u(n+1). \tag{A23}$$

Finally, we compute the new mouthpiece pressure and pressure difference with equations (A13) and (A15). After this, the time index is incremented, and the process is repeated. We note that our numerical formulation is similar to the one proposed in previous studies [5, 9]. However, as pointed out in [24], these formulations amounts to adding a fictitious delay to the system. This artefact is avoided in our formulation; the key-point is to employ a reed oscillator difference equation (equation 8) with a zero instantaneous response.

References

[1] J. Backus: Small-vibration theory of the clarinet. J. Acoust. Soc. Am. **35** (1963) 305–313.

[2] W. E. Worman: Self-sustained nonlinear oscillations of medium amplitude in clarinet-like systems. Dissertation. Case Western Reserve University, 1971.

[3] T. A. Wilson, G. S. Beavers: Operating modes of the clarinet. J. Acoust. Soc. Am. **56** (1974) 653–658.

[4] S. C. Thompson: The effect of the reed resonance on woodwind tone production. J. Acoust. Soc. Am. **66** (1979) 1299–1307.

[5] R. T. Schumacher: *Ab Initio* calculations of the oscillations of a clarinet. Acustica **48** (1981) 71–85.

[6] J. Gilbert, J. Kergomard, E. Ngoya: Calculation of the steady state oscillations of a clarinet using the harmonic balance technique. J. Acoust. Soc. Am. **86** (1989) 35–41.

[7] A. Hirschberg, R. W. A. van de Laar, J. P. Marrou-Maurières, A. P. J. Wijnands, H. J. Dane, S. G. Kruijswijk, A. J. M. Houtsma: A Quasi-stationary Model of Air Flow in the Reed Channel of Single-reed Woodwind Instruments. Acta Acustica **70** (1990) 146–154.

[8] D. Rocchesso, F. Turra: A generalized excitator for real-time sound synthesis by physical model. Proceedings of the Stockholm Musical Acoustics Conference, 1993, 584–588.

[9] B. Gazengel, J. Gilbert, N. Amir: Time domain simulation of single reed wind instrument. From the measured input impedance to the synthesis signal. Where are the traps? Acta Acustica **3** (1995) 445–472.

[10] J. M. Adrien, R. Caussé, E. Ducasse: Dynamic modeling of stringed and wind instruments, sound synthesis by physical models. Proceedings of the 1988 International Computer Music Conference, Köln, 1988, Computer Music Association, 265–276.

[11] E. Ducasse: A physical model of a single-reed wind instrument, including actions of the player. Computer Music Journal **27** (2003) 59–70.

[12] B. Gazengel: Caractérisation objective de la qualité de justesse, de timbre et d'émission des instruments à vent à anche simple. Dissertation. Université du Maine, Le Mans, France, 1994.

[13] M. Roseau: Vibrations in mechanical systems : analytical methods and applications. Springer-Verlag, Berlin, 1987.

[14] W. T. Thomson: Theory of vibration with applications. Stanley Thornes Ltd, Cheltenham, UK, New York, 1972.

[15] R. Stuifmeel: Vibration modes of a metal reed of a reed organ pipe: Theory and experiment. Tech. Rept. Eindhoven University of Technology, 1989.

[16] M. P. de Vries, H. K. Schutt, G. J. Verkerke: Determination of parameters for lumped parameter models of the vocal folds using a finite-difference method approach. J. Acoust. Soc. Am. **106** (1999) 3620–3628.

[17] F. Avanzini, M. van Walstijn: Modelling the mechanical response of the reed-mouthpiece-lip system of a clarinet. Part I. a one-dimensional distributed model. Acta Acustica united with Acustica **90** (2004) 537–547.

[18] J.-P. Dalmont, G. Gilbert, S. Ollivier: Nonlinear characteristics of single-reed instruments: quasistatic volume flow and reed opening measurements. J. Acoust. Soc. Am. **114** (2003) 2253–2262.

[19] C. J. Nederveen: Acoustical aspects of woodwind instruments. Frits Knuf, Amsterdam, The Netherlands, 1969. Revised 1998 Nortern Illinois University Press.

[20] J. O. Smith: Efficient simulation of the reed-bore and bow-string mechanisms. Proceedings of the 1986 International Computer Music Conference, The Hague, Netherlands, 1986, Computer Music Association, 275–280.

[21] P. R. Cook: Non-linear periodic prediction for on-line identification of oscillator characteristics in woodwind instruments. Proceedings of the 1991 International Computer Music Conference, Montreal, Canada, 1991, Computer Music Association, 157–160.

[22] J. O. Smith: Discrete-time modeling of acoustic systems with applications to sound synthesis of musical instruments. Proceedings of the Nordic Acoustical Meeting, Helsinki, 1996, 21–32. Plenary paper.

[23] R. T. Schumacher: Self-sustained oscillations of the clarinet: An Integral Equation Approach. Acustica **40** (1978) 298–309.

[24] F. Avanzini, D. Rocchesso: Efficiency, accuracy, and stbility issues in discrete-time simulations of single reed wind instruments. J. Acoust. Soc. Am. **111** (2002).

[25] M. O. van Walstijn: Discrete-time modelling of brass and reed woodwind instruments with application to musical sound synthesis. Dissertation. Faculty of Music, University of Edinburgh, 2002. http://www.ph.ed.ac.uk/∼maarten/.

[26] P. Guillemain: A digital synthesis model of double-reed wind instruments. EURASIP Journal on Applied Signal Processing **7** (2004) 990–1000.

[27] J. Proakis, D. Manolakis: Digital signal processing. Principles, algorithms, and applications. MacMillan Publishing Company, New York, 1992.

[28] M. O. van Walstijn, D. Campbell: Discrete-time modelling of woodwind instrument bores using wave variables. J. Acoust. Soc. Am. **113** (2003) 575–585.

[29] J. Kergomard: Elementary considerations on reed-instrument oscillations. – In: The Mechanics of Musical Instruments. A. Hirschberg, J. Kergomard, G. Weinreich (eds.). Springer-Verlag, New York, 1995.

[30] A. H. Benade: Fundamentals of musical acoustics. Oxford University Press, New York, 1976.

[31] S. E. Stewart, W. J. Strong: Functional model of a simplified clarinet. J. Acoust. Soc. Am. **68** (1980) 109–120.

[32] N. Bak, P. Dømler: The relation between blowing pressure and blowing frequency in clarinet playing. Acta Acustica **63** (1987) 238–241.

[33] A. Hirschberg, J. Gilbert, A. P. J. Wijnands, A. M. C. Valkering: Musical aero-acoustics of the clarinet. Journal de Physique IV, Toulouse, France, 1994, 559–568. Third French Conference on Acoustics.

[34] F. Pinard, B. Laine, H. Vach: Musical quality assessment of clarinet reeds using optical holography. J. Acoust. Soc. Am. **113** (2003) 1736–1742.